Calcif Tissue Int (2008) 83:425–437
DOI 10.1007/s00223-008-9185-7

LABORATORY INVESTIGATION

Characterization of the Bone Phenotype in ClC-7-Deficient Mice

Anita Vibsig Neutzsky-Wulff · Morten A. Karsdal · Kim Henriksen

Received: 30 July 2008 / Accepted: 4 September 2008 / Published online: 29 October 2008

Abstract Mice deficient in the chloride channel ClC-7, which is likely involved in acidification of the resorption lacuna, display severe osteopetrosis. To fully characterize the osteopetrotic phenotype, the phenotypes of osteoclasts and osteoblasts were evaluated. ClC-$7^{-/-}$ mice and their corresponding wild-type littermates were killed at 4–5 weeks of age. Biochemical markers of bone resorption (CTX-I), osteoclast number (TRAP5b), and osteoblast activity (ALP) were evaluated in serum. Splenocytes were differentiated into osteoclasts using M-CSF and RANKL. Mature osteoclasts were seeded on calcified or decalcified bone slices, and CTX-I, Ca^{2+}, and TRAP were measured. Acidification rates in membrane vesicles from bone cells were measured using acridine orange. Osteoblastogenesis and nodule formation in vitro were investigated using calvarial osteoblasts. ClC-$7^{-/-}$ osteoclasts were unable to resorb calcified bone in vitro. However, osteoclasts were able to degrade decalcified bone. Acid influx in bone membrane vesicles was reduced by 70% in ClC-$7^{-/-}$ mice. Serum ALP was increased by 30% and TRAP5b was increased by 250% in ClC-$7^{-/-}$ mice, whereas the CTX/TRAP5b ratio was reduced to 50% of the wild-type level. Finally, evaluation of calvarial ClC-$7^{-/-}$ osteoblasts showed normal osteoblastogenesis. In summary, we present evidence supporting a pivotal role for ClC-7 in acidification of the resorption lacuna and evidence indicating that bone formation and bone resorption are no longer balanced in ClC-$7^{-/-}$ mice.

Keywords ClC-7 · *Clcn7* · Acidification · Osteopetrosis · Osteoclast · Coupling

A. V. Neutzsky-Wulff · M. A. Karsdal · K. Henriksen (✉)
Nordic Bioscience A/S, Herlev Hovedgade 207, 2730 Herlev, Denmark
e-mail: kh@nordicbioscience.com

A. V. Neutzsky-Wulff
e-mail: avn@nordicbioscience.com

M. A. Karsdal
e-mail: mk@nordicbioscience.com

Bone remodeling is a continuous process, in which old bone matrix is resorbed by the osteoclasts and new bone formation is performed by the osteoblasts. Bone remodeling is important for calcium homeostasis as well as structural integrity of the bones, and during normal bone remodeling, a delicate balance between bone resorption and bone formation, with formation always following resorption, ensures the status quo of the bone mass [1, 2]. This phenomenon, with a tight balance between the two processes, is referred to as "coupling" [1, 2]. If the coupling between resorption and formation is disturbed or out of balance, bone loss (*osteoporosis*) or increased bone mass (*osteopetrosis*) is likely to occur [3, 4].

Osteoclasts resorb the calcified bone matrix or the inorganic part of the bone matrix by lowering pH in the resorption compartment by secretion of hydrochloric acid [3, 5]. Dissolution of the organic part of the bone matrix follows dissolution of the inorganic part of the bone matrix and is dependent on cathepsin K and matrix metalloproteinases (MMPs) [6].

A decrease of pH in the resorption lacuna is facilitated by active transport of protons into the resorption lacunae, which is mediated by an osteoclast specific V-ATPase [3, 5, 7–10]. To obtain electroneutrality, which is essential for maintenance of the low pH, chloride is funneled through chloride channel 7 (ClC-7) [11–13]. Until recently it was unclear whether the transport of Cl^- through ClC-7 occurred passively, as is the case for ClC-1, ClC-2, ClC-

Ka, and ClC-Kb [11, 12, 14], or by Cl^-/H^+ exchange, as is the case for ClC-4, ClC-5, and ClC-e1 [15–17]; but very recent data point toward ClC-7 being a Cl^-/H^+ antiporter [18]. It has been shown that osteopetrosis-associated transmembrane protein 1 (Ostm1) functions as β-subunit for ClC-7 [19], and it has been suggested that Ostm1 has a role in the protein stability of ClC-7 [19]; but the precise role of the interaction between Ostm1 and ClC-7 is not fully elucidated at this point.

Osteopetrosis is in most cases caused by dysfunctional osteoclasts [20–23]. The predominant osteoclast defect leading to osteopetrosis in humans is an inability of the osteoclasts to acidify the resorption lacuna [20, 23], resulting in low or absent resorption. Mutations in either V-ATPase or ClC-7 can lead to this type of osteopetrosis [9, 13, 24]. A special feature associated with this type of osteopetrosis is an apparent uncoupling phenomenon in which the resulting low bone resorption is not followed by low bone formation; in fact, the bone formation appears to be normal or even increased [25–28]. This phenomenon could be explained by the presence of an osteoblast-activating signal deriving directly from the osteoclast and not the resorption itself [28–31].

In this study, a genetically modified mouse strain with a deletion in the *Clcn7* gene encoding ClC-7 [13] was used for the characterization of the bone phenotype. ClC-$7^{-/-}$ mice exhibit a strong osteopetrotic phenotype with a high bone mineral density (BMD), short stature, no eruption of incisors, limited bone marrow space, and splenomegaly [13]. Furthermore, the mice exhibit lysosomal storage disease, neurodegeneration, and retinal degeneration [13, 32]. ClC-$7^{-/-}$ mice live until the age of 6–7 weeks, at which point they die due to the consequences of the severe osteopetrotic phenotype [32].

In this study, we performed a thorough investigation of the bone phenotype, as well as both osteoclasts and osteoblasts derived from osteopetrotic ClC-$7^{-/-}$ mice and their healthy littermates (ClC-$7^{+/?}$). Furthermore, the in vivo levels of dynamic biochemical markers of bone resorption and formation were evaluated.

Materials and Methods

Mice

The genetically engineered ClC-7 mouse strain was kindly provided by Thomas Jentsch (FMP/MDC, Berlin, Germany). The mouse strain was generated by deletion of exons 3–7 in the *Clcn7* gene (construct C7A) as described by Kornak et al. [13].

Pups were given a soft diet (dough diet for transgenic mice [BioServ, Frenchtown, NJ] mixed 1:1 with Solid Drink [Triple A Trading, Tiel, the Netherlands]) each day from P17 until death. After weaning at postnatal day 20, the pups were placed in heated cages. Mice were killed at 4–5 weeks of age. At the time of death, a full bleed was performed. Prior to a full bleed, mice were fasted for 12 hours.

Digital Histographs

Digital histographs were captured using an Olympus (Tokyo, Japan) DP71 digital camera mounted on an Olympus IX-70 or an Olympus BX-60 microscope, equipped with ×2, ×4, ×10, ×20, ×60, and ×100 objectives.

Tissue Fixation, Embedding, and Sectioning

For plastic sections, vertebrae and femurs were fixed in 70% ethanol and then embedded in methylmethacrylate in a fully calcified state. Longitudinal sections of 7 µM thickness were cut using the Microm HM360 (Microm International, Walldorf, Germany).

For paraffin sections, vertebrae and femurs were fixed in 3.7% formaldehyde in PBS, decalcified in 15% EDTA, dehydrated, and embedded in paraffin. Sections of 5 µM thickness were cut using the Microm HM360.

Histological Staining on Paraffin Sections

Prior to each staining, paraffin sections were deparaffinized by heating at 60°C for 30 minutes and sequential hydration (toluene → 99% ethanol → 96% ethanol → 70% ethanol → H_2O). After each staining, unless stated otherwise, sections were dehydrated (70% ethanol → 96% ethanol → 99% ethanol → toluene) and mounted with dextropropoxyphene (DPX).

Alcian Blue Staining of Cartilage

After deparaffinization, sections were placed in alcian blue solution (1% alcian blue in 3% acetic acid solution, pH 2.5, filtered before use) for 30 minutes, then in running water for 2 minutes. Sections were afterward placed in Mayer's hematoxylin (Bie & Berntsen, Rødovre, Denmark) for 5 minutes and finally placed in running water for 1 minute, dehydrated and mounted.

Toluidine Blue Staining of Cartilage

After deparaffinization, sections were placed in toluidine blue solution (0.05% toluidine blue in McIlvaine's buffer) for 2 minutes. Sections were washed in McIlvaine's buffer (1.4% disodium hydrogen phosphate dehydrate, 1.3% citric acid, pH 4) for 10 seconds. Sections were carefully dried with filter paper and subsequently dried for 1 hour at 37°C. Sections were placed directly in toluene for 5 minutes, followed by mounting.

TRAP Activity: Staining of Osteoclasts

Tartrate-resistant acid phosphatase (TRAP) activity was identified as previously described [33].

Histological Staining on Plastic Sections

Prior to each staining method, plastic sections were deplastified and hydrated (2-methoxy-ethylacetate → 99% ethanol → 96% ethanol → 70% ethanol → H_2O). After each staining, unless stated otherwise, sections were dehydrated and mounted with DPX.

von Kossa Staining of Mineralized Bone Tissue

After deplastification and hydration, sections were washed several times in Milli Q water (Millipore, Bedford, MA). Sections were transferred to 1% silver nitrate for 5 minutes, and the staining was developed in 1% pyrogallol for 5 seconds. Sections were transferred to 1% sodium thiosulfate for 5 minutes and washed, followed by dehydration and mounting.

Generation of Osteoclasts from Spleen

Spleens were dissected from dead mice, and all soft connective tissue was removed. Spleens were mashed through a 70-μm nylon mesh, while using α-minimum essential medium (αMEM, supplemented with thymidine 388 μg/L, penicillin/streptomycin 100 units/ml of each) to wash the cells through the mesh. The cell suspension was carefully loaded on Lymphocyte Separation Medium (ICN Biomedicals, Costa Mesa, CA) and centrifuged for 20 minutes at 2,000 rpm, without break. The layer of cells at the interface was collected, washed twice in αMEM, and resuspended in osteoclast differentiation medium containing αMEM (supplemented with thymidine 388 μg/L, penicillin/streptomycin 100 units/ml of each) with addition of 10% heat-inactivated (HI) fetal bovine serum and 30 ng/ml macrophage colony-stimulating factor (M-CSF) (216-MC; R&D Systems, Minneapolis, MN). Mouse receptor activator of NF-κB ligand (RANKL; 462-TR, R&D Systems) at a concentration of 100 ng/ml was added either at the beginning of the culture period or after 4 days of culture. Medium containing both M-CSF and RANKL is hereafter referred to as "MOC med."

Osteoclastogenesis Experiment

Isolated spleen cells were seeded on calcified bone slices at a density of 250,000/cm^2 and cultured in MOC med for 12 days. Medium was changed every 2–3 days, and culture supernatants were collected and stored at −20°C until further analysis.

Bone Resorption by Mature Osteoclasts

Isolated spleen cells were differentiated into mature osteoclasts by, first, 4 days of culture without RANKL, lifting by trypsinization, and reseeding at a cell density of 900,000/six-well, followed by 7 days of culture in MOC med with medium exchange every day. Mature osteoclasts from either genotype were lifted using trypsin and cell scraping and then reseeded on either calcified or decalcified bone slices at a density of 50,000/bone slice. Cells were cultured in MOC med for 3 days, with a change of medium every day. Culture supernatants were collected and stored at −20°C until further analysis.

Osteoclasts for Morphological Evaluation

Mature osteoclasts from either genotype were lifted using trypsin and cell scraping and then reseeded on plastic at a density of 50,000/96-well. Cells were cultured in MOC med for 3 days, with a change of medium every day. At day 3, cells were fixed in 3.7% formaldehyde in PBS.

Bone Slices

Sticks of cortical bone from cows were cut into thin slices (0.5 cm diameter). The slices were kept in 70% ethanol until use. Some of the bone slices were decalcified prior to experiments. This was achieved by placing the bone slices in 15% EDTA for 1 week, with exchange of EDTA each day, as described previously [6]. Prior to the seeding of cells, bone slices were washed thoroughly in the appropriate medium.

Measurement of TRAP Activity in Cell Culture Supernatants

TRAP activity in cell culture medium was measured as described previously by Karsdal et al. [29]. Briefly, samples were incubated with TRAP reaction buffer, containing *p*-nitrophenyl phosphate and sodium tartrate [29], for 1 hour at 37°C in the dark. Reaction was stopped with 0.3 M NaOH. Absorbance was measured in an ELISA reader at 405 nm with 650 nm as reference.

Measurement of MMP Activity in Cell Culture Supernatants

MMP activity was measured in supernatants as previously described by Ridnour et al. [34], with small modifications. Briefly, samples and buffer (0.01 M $CaCl_2$, 0.2 M NaCl,

0.05 M Tris-HCl, 50 μM $ZnSO_4$, 0.05% Brij) were mixed. The MMP substrate Mca-Pro-Leu-Gly-Leu-Dap(Dnp)-Ala-Arg-NH_2 (M-1895; Bachem, Bubendorf, Switzerland), was added at a final concentration of 2 μM and incubated at 37°C for 20 minutes. Fluorescence was measured at excitation 328 nm and emission 392 nm. MMP activity in medium collected from bone slices without cells was used as background.

Gelatinase Zymography

Gelatinase activity in culture supernatants was tested by gelatinase zymography as previously described [35]. MMP-2 and MMP-9 were used as markers.

Measurement of Bone Degradation by CTX-I in Serum and Cell Culture Supernatants

Bone degradation was measured in serum by measurement of C-terminal type I collagen fragments (CTX-I) by the RatLaps ELISA (1RTL4000; IDS, Herlev, Denmark). The CTX-I concentration in cell culture supernatants was measured by the CrossLaps for culture ELISA (6CRL4000, IDS). Both ELISAs were performed according to the manufacturer's protocol.

Measurement of Bone Degradation by Calcium Release

The concentration of total calcium was measured in 100-μL culture supernatants by a colorimetric assay using the Advia 1800 (Siemens, Munich, Germany). Measurements of calcium release from cells on plastic were used as background.

Staining and Counting of Pits

Cells were removed from bone slices by cotton swabs, followed by three rounds of washing of the bone slices in Milli Q water. Resorption pits were stained with filtered Mayers hematoxylin for 8 minutes while shaking. Bone slices were rinsed three times in Milli Q water and finally cleaned with a cotton swab to remove excess dye. Stained pits were counted using the CAST program (Olympus, Glostrup, Denmark). The resorbed area on each bone slice was calculated according to the settings in the program.

TRAP Staining of Cells

Fixed osteoclasts were TRAP-stained using the leukocyte acid phosphatase kit (Sigma-Aldrich, St. Louis, MO) according to the manufacturer's protocol. The number of TRAP-positive cells was counted using the CAST program, or digital histographs were taken.

Phalloidin and DAPI Staining of Fixed Osteoclasts

Staining of fixed osteoclasts with tetramethyl-rhodamine isothiocyanate (TRITC)–conjugated phalloidin and 4,6-diamidino-2-phenylindole (DAPI) was performed as described by Karsdal et al. [30]. Digital histographs were taken using filters suitable for TRITC and DAPI. The pictures were overlayed using ImagePro software (Media Cybernetics, Silver Spring, MD).

Isolation of Bone Microsomes

Whole bones were isolated from 4-week-old mice, and all non-bone-related tissues were removed. Bones were placed in isolation buffer containing Complete EDTA-free protease blockers (Roche, Indianapolis, IN), homogenized using a polytron blender, and further homogenized using a Teflon homogenator. Homogenates were centrifuged for 15 minutes at 10,000*g* and the supernatants collected. Supernatants were then centrifuged for 60 minutes at 100,000*g* and the pellets collected and resuspended in isolation buffer; protein concentrations were determined using the DC Protein Asssay (Bio-Rad, Richmond, CA).

Influx Assay

The influx assay was performed as previously described [8, 36, 37]. Briefly, bone microsomes were incubated in reaction buffer (5 mM HEPES, 150 mM KCl, 5 mM $MgSO_4$, 15 μM acridine orange, and 1 μM valinomycin, pH 7.2). The reaction was incubated at room temperature for 30 minutes to obtain a steady state in temperature, dye uptake, and background fluorescence. Then, the reaction was initiated by addition of ATP (final concentration 5 mM), and immediately afterward the plate was read using excitation at 492 nm and emission at 535 nm. Fluorescence was read every 15 seconds for 3 minutes. The results are presented as the slope of the influx curves, which is calculated as the change in fluorescence emission (ΔF) as a function of the change in time (Δt) over the entire 3-minute time span.

Immunoblotting

To evaluate levels of protein expression, 30 μg of whole-bone microsomes from either ClC-$7^{+/?}$ or ClC-$7^{-/-}$ mice were run on an SDS-PAGE gel and electroblotted. The various proteins were detected using one of the following primary antibodies: rabbit antibody against ClC-7 [13], against the B1/B2 subunit of V-ATPase (Santa Cruz Biotechnology, Santa Cruz, CA), and ß-actin (Sigma-Aldrich), with B1/B2 and ß-actin being internal controls. The corresponding secondary antibodies were used, and all blots

were visualized using the ECL kit from Amersham Bioscience (Arlington Heights, IL) as described by Henriksen et al. [38]. To ensure that equal amounts of protein were loaded, ponceau red staining was used [38].

Measurement of TRAP5b Activity in Serum

TRAP5b activity in serum was measured by the Mouse-TRAP assay (SD-TR103, IDS). The assay was performed according to the manufacturer's protocol. Serum samples from individual mice were diluted in PBS to suitable dilutions in order to obtain readings within the range of the kit.

Measurement of ALP in Serum

Alkaline phosphatase (ALP) was measured by mixing serum samples or controls with substrate solution (0.95 ml AMP buffer [50 ml Milli Q water, 6.25 ml 2-amino-2-methyl-1-propanol 95% {A65182, Sigma}, pH adjusted to 10.0, volume adjusted to 62.5 ml by addition of Milli Q water], 9.5 ml Milli Q water, 40 mg PNPP [P5994, Sigma], 190 µL 1 M $MgCl_2$) and incubating for 20 minutes in the dark. The reaction was stopped by addition of 0.5 M NaOH. Colorimetric changes were measured at 405 nm with 650 nm as reference using an ELISA reader.

Generation and Differentiation of Primary Osteoblasts

Primary osteoblasts were obtained by dissection of calvariae from pups 4–5 weeks old. Calvariae were rinsed in PBS and afterward minced thoroughly with a pair of scissors in αMEM. Minced calvariae were transferred to culture flasks containing αMEM with 10% HI bovine serum. Cultures were grown until confluence, lifted, reseeded at a density of 25,000 cells/24-well, and grown for 3 weeks in medium supplemented with 50 µg/ml ascorbic acid and 10 mM β-glycerol phosphate, in the absence or presence of bone morphogenetic protein-2 (BMP-2, 100 ng/ml). Medium was changed every 2–3 days.

Alamar Blue for Assessment of Cell Viability

Measurements of cell viability were performed by the Alamar blue assay (Biosource, Camarillo, CA). αMEM with 10% Alamar blue was added to wells with living cells and empty wells (for background) and incubated at 37°C until a change of color from blue to purple/red had occurred (1–5 hours). After incubation, fluorescence was measured at excitation 540 nm and emission 590 nm in a fluorescence reader.

Alizarin Red Staining of Bone Nodules

Fixed cells were stained with 40 mM alizarin red-S (pH 4.2) for 10 minutes with shaking. Wells were washed in Milli Q water, followed by washing in PBS while shaking.

Dye extraction was performed with 10% cetylpyridinum chloride (500 µL/24-well) by incubation overnight in the dark with shaking. Absorbance was subsequently measured at 561 nm in an ELISA reader.

Statistics

All statistical calculations were performed by Student's two-tailed unpaired *t*-test, assuming normal distribution and equal variance, with a significance level of $P = 0.05$ (NS, not significant; $*P < 0.05$, $**P < 0.01$, $***P < 0.001$). Error bars indicate standard error of the mean (SEM).

Results

ClC-7-Deficient Mice Show Osteoclast-Rich Severe Osteopetrosis

The bone phenotype of ClC-7 deficient mice was evaluated by von Kossa staining and, as seen in Fig. 1 (a2 and a4), the mice exhibit a very severe osteopetrotic phenotype. To examine whether this effect is due to malfunctioning osteoclasts or to increased osteoblast activity, staining of cartilage was performed. Figure 1 (b1–b6) shows high levels of remaining cartilage in ClC-$7^{-/-}$ bones, as evidenced by alcian blue (b1, b2) and toluidine blue (b3–b6) staining, indicating that the phenotype is due to defective osteoclasts.

To characterize the osteoclast phenotype of ClC-$7^{-/-}$ mice further, staining of the osteoclast marker TRAP in bone sections was performed; and as seen in Fig. 1c2, a large part of the bone surface in ClC-$7^{-/-}$ mice was covered with TRAP-positive cells, compared to ClC-$7^{+/?}$ mice (Fig. 1c1). Furthermore, osteoclasts in ClC-$7^{-/-}$ mice appear to deposit TRAP on the adjacent bone surfaces, as seen in Fig. 1c4. TRAP deposition is also present in ClC-$7^{+/?}$ mice but to a much lower extent (Fig. 1c3). Furthermore, ClC-$7^{-/-}$ osteoclasts in vivo seem to be flatter and more stretched compared to ClC-$7^{+/?}$ osteoclasts (Fig. 1c3, c4).

ClC-$7^{-/-}$ Osteoclasts Do Not Show Signs of Resorption, Despite Normal Osteoclast Differentiation

To address whether murine ClC-$7^{-/-}$ osteoclasts have normal differentiation, in vitro experiments were performed

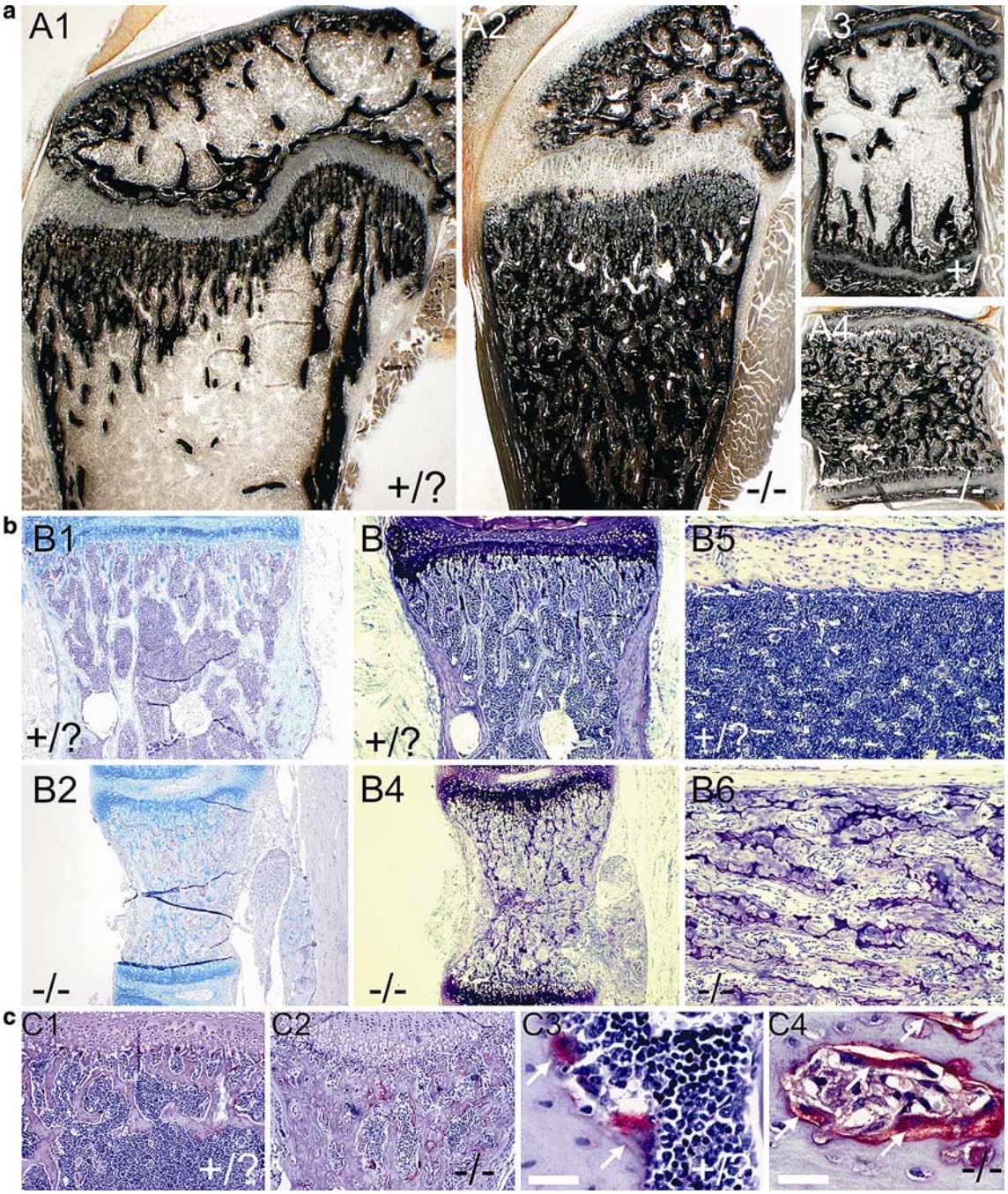

Fig. 1 ClC-7-deficient mice show osteoclast-rich osteopetrosis. Mice were killed at 4–5 weeks of age. Femora and vertebrae were dissected, fixed, embedded in plastic or paraffin, and sectioned. **a** Von Kossa staining of plastic sections. **a1** Femur from ClC-$7^{+/?}$ mouse. **a2** Femur from ClC-$7^{-/-}$ mouse. **a3** Vertebra from ClC-$7^{+/?}$ mouse. **a4** Vertebra from ClC-$7^{-/-}$ mouse. **b** Staining of cartilage on paraffin sections. **b1**, **b2** Alcian blue staining of vertebrae. **b3**, **b4** Toluidine blue staining of vertebrae. **b5**, **b6** Higher magnification of toluidine blue–stained sections of femora. Histographs were taken in the shaft area of the femur. **c** TRAP staining of paraffin sections. **c1**, **c2** Vertebrae. Magnification ×10. **c3**, **c4** High magnification of osteoclasts. Multinucleated osteoclasts are indicated with *arrows*. Scale bars = 30 μm

to assess osteoclast differentiation and the ability of the cells to resorb bone. Firstly, TRAP activity increased throughout the culture period, as expected [39], and only minor differences between ClC-$7^{+/?}$ and ClC-$7^{-/-}$ cells were observed during differentiation (Fig. 2a). Furthermore, only slight differences in gelatinase activity were shown between ClC-$7^{+/?}$ and ClC-$7^{-/-}$ cells (Fig. 2b). These slight differences are most likely caused by difficulties in performing exactly homogeneous osteoclastogenesis experiments [39, 40]. However, evaluation of bone resorption by measurement of CTX-I and scoring of resorption pits showed that ClC-$7^{-/-}$ osteoclasts have a highly reduced capability for

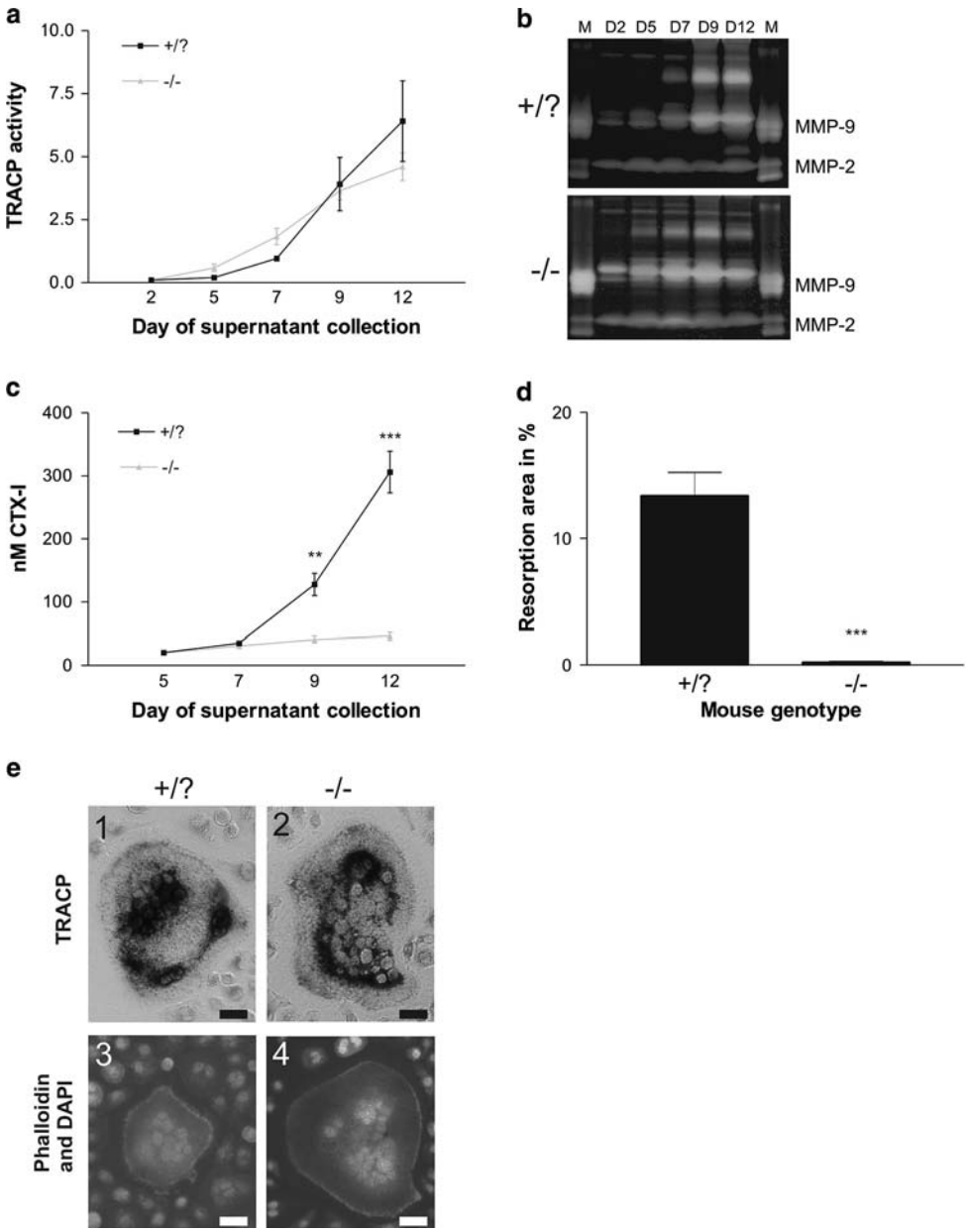

Fig. 2 ClC-7$^{-/-}$ osteoclasts do not resorb, despite normal differentiation. Mice were killed at 4–5 weeks of age. Spleen cells from ClC-7$^{-/-}$ and ClC-7$^{+/?}$ littermates were seeded on calcified bone slices at a density of 250,000/cm^2 and cultured in MOC med from day 0. For morphological studies of osteoclasts on plastic, spleen cells were cultured until mature osteoclasts were present (7 days of culture in MOC med). Cells were seeded on plastic at a density of 50,000/96-well and fixed after 3 days of culture. **a** Accumulated TRAP activity measured in supernatants from cells on bone. **b** Gelatinase zymography measuring MMP activity in supernatants from cells on bone. **c** Accumulated CTX-I measured in supernatants from cells on bone. **d** Resorption pits were stained and the pit area was scored. **e** Staining of osteoclasts on plastic. **e1**, **e2** Staining of TRAP activity. **e3**, **e4** Phalloidin and DAPI staining (overlay pictures). Scale bars = 20 μm. $^{**}P < 0.01$, $^{***}P < 0.001$

resorption of bone (Fig. 2c, d). Finally, the morphology of ClC-7$^{+/?}$ and ClC-7$^{-/-}$ osteoclasts in vitro was examined; and the overall morphology, actin ring formation, as well as TRAP activity were comparable, as seen in Fig. 2 (e1–e4), in line with a previous study [13].

ClC-7$^{-/-}$ Osteoclasts are Unable to Resorb Inorganic Bone Matrix but Able to Resorb Organic Bone Matrix In Vitro

As the investigations of the in vitro morphology of the mature osteoclast did not explain the inability of the ClC-7$^{-/-}$ osteoclasts to resorb bone, further characterization of the functionality of mature ClC-7$^{-/-}$ osteoclasts was performed. An assessment of the ability of mature ClC-7$^{-/-}$ osteoclasts to resorb decalcified bone, compared to normal calcified bone, was conducted. Firstly, bone resorption was measured by CTX-I, and as seen in the differentiation experiment (Fig. 2c, d), ClC-7$^{-/-}$ osteoclasts showed no indication of resorption on calcified bone slices (Fig. 3a). Interestingly, resorption of decalcified bone slices was mildly, but nonsignificantly, reduced in ClC-7$^{-/-}$ osteoclasts compared to ClC-7$^{+/?}$ osteoclasts (Fig. 3a). These results were further supported by measurements of calcium released during bone resorption of the calcified bone slices, which was strongly reduced in ClC-7$^{-/-}$ osteoclasts compared to ClC-7$^{+/?}$ osteoclasts (Fig. 3b). We then scored the number of osteoclasts and

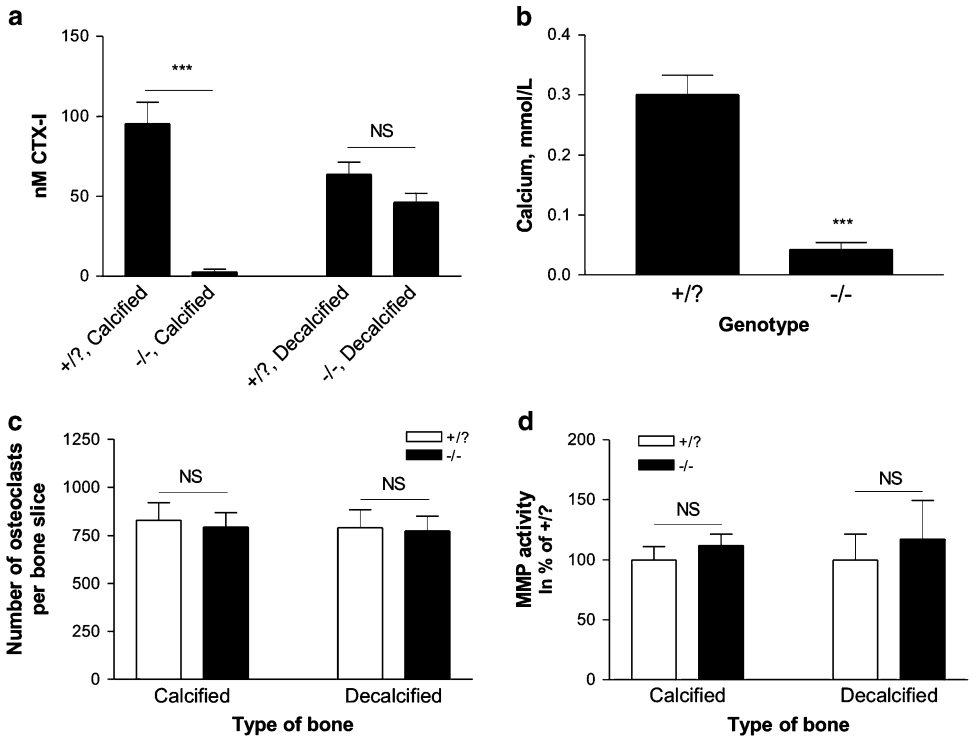

Fig. 3 ClC-$7^{-/-}$ osteoclasts can degrade organic matrix but do not resorb inorganic matrix. Mice were killed at 4–5 weeks of age. Spleen cells from ClC-$7^{-/-}$ and ClC-$7^{+/?}$ littermates were cultured until mature osteoclasts were present (7 days), after which they were seeded at a density of 50,000/96-well on calcified or decalcified bone slices, grown for 3 days and fixed. **a** Bone resorption measured by CTX-I in culture supernatants from day 3. **b** Bone resorption measured by calcium release to culture supernatants from cells on calcified bone. **c** Counting of TRAP-positive cells. **d** Measurement of MMP activity in culture supernatants from day 3. Results are standardized to levels of ClC-$7^{+/?}$ on either type of bone. NS, nonsignificant; $^{**}P < 0.01$

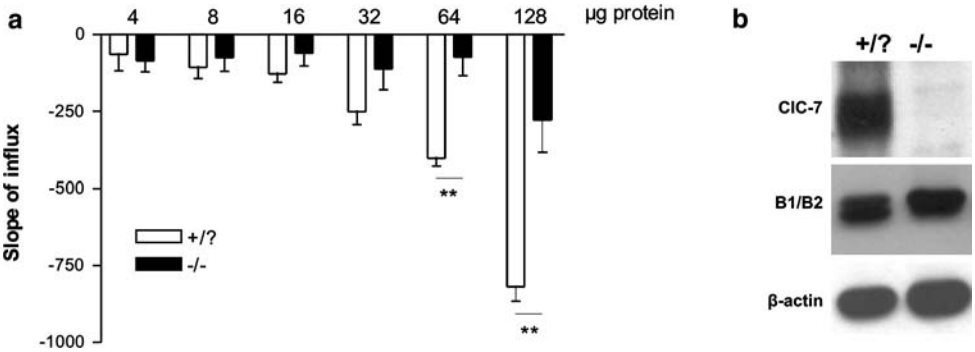

Fig. 4 ClC-7-deficient bone cells show decreased acidification potential. Bone microsomal vesicles from ClC-$7^{-/-}$ and ClC-$7^{+/?}$ mice were isolated. **a** Acid influx was quantified as described in "Materials and Methods." **b** Bone microsomes (30 µg) were immunoblotted and tested for expression of ClC-7, the B1/B2 subunits of V-ATPase, and β-actin. $^{**}P < 0.01$

found no changes in either the number of TRAP-positive multinucleated cells or MMP activity (Fig. 3c, d). Taken together, these results strongly indicate that the bone resorption defect is caused by an inability of the osteoclasts to resorb the inorganic part of the bone matrix, thereby supporting a role for ClC-7 in acidification of the resorption lacuna.

ClC-7 Deficiency Results in Decreased Acidification of Bone Membrane Vesicles

To investigate the acidification of membrane vesicles deriving from bone cells of ClC-$7^{-/-}$ and ClC-$7^{+/?}$ mice, we generated whole-bone microsomes and investigated the acid influx in these fractions. Firstly, we investigated acid influx in the microsomes and, as can be seen in Fig. 4a, found that the ClC-$7^{+/?}$ fractions showed acid influx even at low protein concentrations, whereas the ClC-$7^{-/-}$ fractions only showed acid influx at the highest concentration of microsomes investigated; at this concentration the influx was about 30% of that seen in the ClC-$7^{+/?}$ fractions. We then examined ClC-7 expression in the microsomes and, as can be seen in Fig. 4b, found high expression in the ClC-$7^{+/?}$ microsomes and complete absence of the 80-kDa ClC-7 band in the ClC-$7^{-/-}$ microsomes. To ensure correct loading of the membranes, we tested expression of both the B1 and B2 subunits of V-ATPase and of β-actin and found no differences in the expression of any of these proteins (Fig. 4b), confirming that the main difference in the microsomes was the presence or absence of ClC-7. These data support a role for ClC-7 in the acidification of the lysosomes and the resorption lacunae.

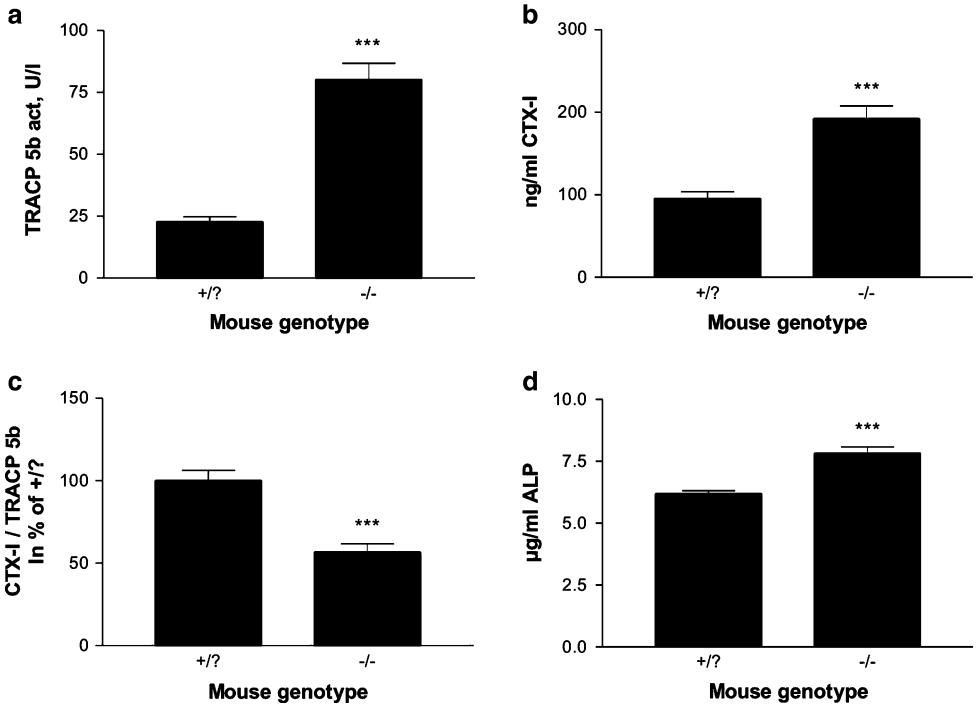

Fig. 5 ClC-$7^{-/-}$ osteoclasts resorb less in vivo. Mice were fasted 12 hours prior to death at 4–5 weeks of age, and a full bleed was performed. Serum samples were isolated and various bone markers were measured. **a** Relative number of osteoclasts measured by TRAP5b activity. **b** Bone resorption measured by CTX-I. **c** Bone resorption per osteoclast (CTX-I/TRAP5b). **d** Measurements of ALP. ***$P < 0.001$

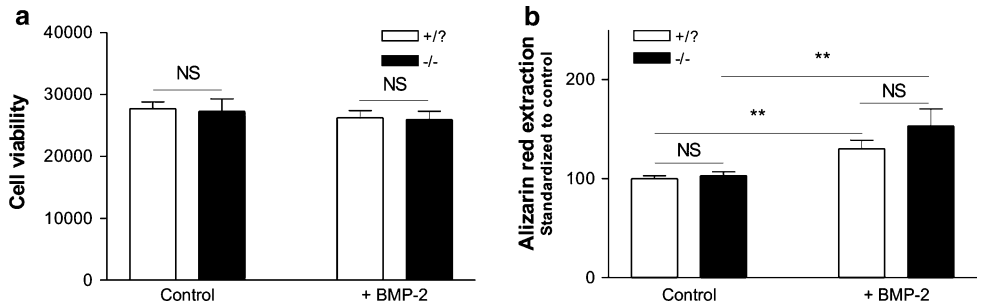

Fig. 6 Osteogenic properties of ClC-$7^{-/-}$ osteoblasts are normal. Mice were killed at 4–5 weeks of age. Calvariae from ClC-$7^{-/-}$ and ClC-$7^{+/?}$ mice were dissected. Calvarial osteoblasts were cultured for 14 days in osteogenic medium, with or without BMP-2 (100 ng/ml). **a** Cell viability measured by Alamar blue at day 14. **b** Dye extraction of alizarin red–stained nodules. Results are standardized to control ClC-$7^{+/?}$ cells. NS, nonsignificant; **$P < 0.01$

ClC-$7^{-/-}$ Mice have Decreased Resorption Per Osteoclast and Increased Bone Formation Markers In Vivo

We examined the number and activity of osteoclasts in vivo by measuring TRAP and CTX-I. TRAP5b activity showed that the number of osteoclasts was increased by more than 200% in ClC-$7^{-/-}$ mice (Fig. 5a). Measurements of CTX-I, surprisingly, indicated increased resorption in ClC-$7^{-/-}$ mice (Fig. 5b). However, to evaluate the function of the individual osteoclasts, the absolute resorption should be correlated to the number of osteoclasts in the mice [41]. When this aspect was addressed, a highly significant decrease in resorption per osteoclast, to 50% of the ClC-$7^{+/?}$ mice value, was observed for ClC-$7^{-/-}$ mice (Fig. 5c).

To address whether bone formation was affected by the lack of ClC-7 in vivo, the bone formation marker ALP was also measured in serum. The results showed a significant increase in the ALP level for ClC-$7^{-/-}$ mice compared to healthy littermates (Fig. 5d). These results indicate an apparent ongoing bone formation in ClC-7-deficient mice, despite the strongly reduced resorption per osteoclast.

No Enhanced Osteogenic Effect of ClC-7-Deficient Osteoblasts In Vitro

To examine whether intrinsic changes in ClC-$7^{-/-}$ osteoblasts caused the apparent ongoing bone formation in ClC-7-deficient mice, the ability of both ClC-$7^{-/-}$ and ClC-$7^{+/?}$ calvarial osteoblasts to perform bone formation was evaluated. No differences in cell viability were observed

(Fig. 6a). Bone nodule formation was examined, showing that BMP-2 induced nodule formation in both ClC-7$^{-/-}$ and ClC-7$^{+/?}$ osteoblasts to the same extent and that the basal bone formation level, without BMP-2 induction, was also equivalent for ClC-7$^{-/-}$ and ClC-7$^{+/?}$ osteoblasts (Fig. 6b). This indicates that the osteoblast phenotype is not altered by the lack of ClC-7.

Discussion

Loss of ClC-7 or mutation in ClC-7 leads to osteopetrosis in both humans and mice due to defective osteoclasts [13, 24, 42, 43], but there has been some dispute about why the lack of ClC-7 leads to defective osteoclasts. ClC-7$^{-/-}$ osteoclasts from mice have previously been shown reduced resorption of ivory in vitro as well as reduced acidification of the resorption compartment [13], and the same has been observed for osteoclasts deriving from patients suffering from autosomal dominant osteopetrosis type II (ADOII), who have a dominant negative mutation in ClC-7 [29, 44]. However, other groups have not observed decreased acidification in ADOII osteoclasts [45], potentially due to the heterogeneous phenotypes seen in ADOII patients [27, 45]. Apart from ClC-7 having a role in acidification of the resorption lacuna, there are alternative theories regarding the role of ClC-7; e.g., a role for ClC-7 in degradation of the organic bone matrix rather than the inorganic bone matrix has been hypothesized [46], and a more motile phonotype of ADOII osteoclasts [47] as well as a less motile phenotype [45] have been observed.

In this study, ClC-7-deficient mice, which have an osteopetrotic phenotype mimicking human autosomal recessive osteopetrosis (ARO) [13, 24, 43], were thoroughly investigated to shed light on the pressing question regarding the exact role of ClC-7 and to investigate the apparent imbalance between bone resorption and bone formation observed in some forms of osteopetrosis [28].

Our initial investigations confirmed the severe osteopetrotic phenotype as seen by the presence of massive amounts of calcified bone matrix in both vertebrae and femora, which is in agreement with Kornak et al. [13]. Furthermore, we also observed high levels of nonresorbed calcified cartilage, and very high numbers of osteoclasts covering a large part of the bone surfaces, in accordance with previous studies [21]. An increased number of osteoclasts is in agreement with an increased survival of osteoclasts when acidification is attenuated, as described previously [29, 38, 48]. Thus, as expected [13], these mice fit perfectly with the "classical" osteopetrotic phenotype caused by defective bone resorption due to malfunctioning osteoclasts [20–23]. Interestingly, the bone surfaces below the osteoclasts were covered in a TRAP-positive material, a yet to be explained phenomenon which is also seen in ClC-7-deficient ADOII patients [42, 49].

When investigating osteoclastogenesis and morphology of the ClC-7$^{-/-}$ osteoclasts in vitro, we found that both parameters were comparable to wild type. This is in line with studies of osteoclastogenesis and morphology in ClC-7-deficient human osteoclasts [43, 44] and morphological studies in ClC-7$^{-/-}$ mice [13].

When investigating resorptive capacity, we found that ClC-7$^{-/-}$ osteoclasts, both under differentiating conditions and as mature osteoclasts, were unable to resorb calcified bone matrix, measured by CTX-I, calcium release, and pit formation, in agreement with results obtained by Kornak et al. [13]. Interestingly, when mature ClC-7$^{-/-}$ osteoclasts were seeded on decalcified bone matrix, they were able to degrade this matrix to a similar level as ClC-7$^{+/?}$ osteoclasts, indicating that resorption of the inorganic part of the bone matrix is hindered whereas resorption of the organic part of the bone matrix is not. We did, however, observe a nonsignificant reduction in the degradation of decalcified bones, which correlates well with our findings using ADOII osteoclasts that showed a minor reduction in the degradation of decalcified bones as well [6]. All these data support the theory that the resorption defect is caused by diminished acidification of the resorption lacuna [13, 29, 37, 44].

To fully elucidate the underlying mechanism causing the reduced resorption, we evaluated acid influx in bone microsomes isolated from both ClC-7$^{-/-}$ and ClC-7$^{+/?}$ mice by use of the dye acridine orange, which is sensitive to changes in pH at the levels observed in lysosomes and the resorption lacuna [7, 36, 50]. In alignment with a role for ClC-7 in acidification of the resorption lacuna/lysosomes, acid influx was strongly attenuated in ClC-7$^{-/-}$ microsomes. As ClC-7 in bone only is expressed in high amounts by osteoclasts [51], the difference in acidification likely reflects the differences in the osteoclasts. These data do not, however, correlate with another study of lysosomal pH performed in ClC-7$^{-/-}$ neurons [32]. However, in this study static pH measurements were performed [32], whereas our pH measurements were dynamic. In addition, the difference between neurons and osteoclasts most likely plays a role. However, our findings correlate well with the recent finding that ClC-7 mediates Cl^-/H^+ antiport transport in liver preparations [52].

Our in vivo analyses of ClC-7-deficient mice showed a highly interesting phenomenon, namely, that resorption per osteoclast was reduced whereas the bone formation marker ALP was increased compared to healthy littermates. The reason for the high CTX-I values observed in ClC-7$^{-/-}$ mice is somewhat puzzling; however, as these mice are still young at time of death, it is likely that the measured increase in CTX-I is attributable to a developmental effect in which MMPs could be responsible for generation of

CTX-I [53]. In fact, high levels of CTX-I are also found in cathepsin K–deficient mice [54], despite the fact that CTX-I release from calcified bone matrix, by the osteoclasts, requires cathepsin K activity [6, 53]. This could indicate that the high level of CTX-I in ClC-$7^{-/-}$ mice originates from the development of the bones, where MMP activity plays a role in degrading the immature bone matrix [55].

Ongoing bone formation in ClC-$7^{-/-}$ mice in vivo was shown by increased levels of ALP in serum, and in vitro analysis of nodule formation by ClC-$7^{-/-}$ osteoblasts demonstrated no intrinsically increased bone formation by these osteoblasts. The finding that bone formation is ongoing in the face of decreased resorption per osteoclast correlates well with recent findings indicating that osteoclasts, independent of resorption, are sources of anabolic signals for osteoblasts [28–31].

In conclusion, we found that ClC-$7^{-/-}$ osteoclasts were unable to resorb calcified bone but were able to resorb decalcified bone. Together with signs of diminished acidification in bone microsomes, our findings support the hypothesis that the defective resorption in ClC-7-deficient mice is due to strongly attenuated acid secretion by osteoclasts. Furthermore, by evaluation of serum markers we found that bone formation is not coupled to resorption in these mice, supporting the view that osteoclasts are sources of bone anabolic signals for osteoblasts and thereby explaining the apparent uncoupling phenotype also observed in osteopetrotic patients.

Acknowledgments We thank Thomas J. Jentsch and Jens Fuhrmann (FMP/MDC, Berlin, Germany) for providing the genetically engineered ClC-7 mouse strain and for critical reading and valuable discussions. We also thank Uwe Kornak (Max Planck Institute for Molecular Genetics, Charité University Hospital, Berlin, Germany) for critical reading and valuable discussions.

References

1. Martin TJ (1993) Hormones in the coupling of bone resorption and formation. Osteoporos Int 3(Suppl 1):121–125
2. Martin TJ, Rodan GA (2001) Coupling of bone resorption and formation during bone remodeling. In: Marcus R, Feldman D, Kelsey J (eds) Osteoporosis, 2nd edn. Academic Press, San Diego, pp 361–370
3. Goltzman D (2002) Discoveries, drugs and skeletal disorders. Nat Rev Drug Discov 1:784–796
4. Teitelbaum SL, Ross FP (2003) Genetic regulation of osteoclast development and function. Nat Rev Genet 4:638–649
5. Roodman GD (1999) Cell biology of the osteoclast. Exp Hematol 27:1229–1241
6. Henriksen K, Sorensen MG, Nielsen RH, Gram J, Schaller S, Dziegiel MH, Everts V, Bollerslev J, Karsdal MA (2006) Degradation of the organic phase of bone by osteoclasts: a secondary role for lysosomal acidification. J Bone Miner Res 21:58–66
7. Baron R, Neff L, Louvard D, Courtoy PJ (1985) Cell-mediated extracellular acidification and bone resorption: evidence for a low pH in resorbing lacunae and localization of a 100-kD lysosomal membrane protein at the osteoclast ruffled border. J Cell Biol 101:2210–2222
8. Blair HC, Teitelbaum SL, Ghiselli R, Gluck S (1989) Osteoclastic bone resorption by a polarized vacuolar proton pump. Science 245:855–857
9. Frattini A, Orchard PJ, Sobacchi C, Giliani S, Abinun M, Mattsson JP, Keeling DJ, Andersson AK, Wallbrandt P, Zecca L, Notarangelo LD, Vezzoni P, Villa A (2000) Defects in TCIRG1 subunit of the vacuolar proton pump are responsible for a subset of human autosomal recessive osteopetrosis. Nat Genet 25:343–346
10. Vaananen HK, Karhukorpi EK, Sundquist K, Wallmark B, Roininen I, Hentunen T, Tuukkanen J, Lakkakorpi P (1990) Evidence for the presence of a proton pump of the vacuolar H^+-ATPase type in the ruffled borders of osteoclasts. J Cell Biol 111:1305–1311
11. Jentsch TJ (2007) Chloride and the endosomal–lysosomal pathway: emerging roles of CLC chloride transporters. J Physiol 578:633–640
12. Jentsch TJ, Stein V, Weinreich F, Zdebik AA (2002) Molecular structure and physiological function of chloride channels. Physiol Rev 82:503–568
13. Kornak U, Kasper D, Bosl MR, Kaiser E, Schweizer M, Schulz A, Friedrich W, Delling G, Jentsch TJ (2001) Loss of the ClC–7 chloride channel leads to osteopetrosis in mice and man. Cell 104:205–215
14. Jentsch TJ, Neagoe I, Scheel O (2005) CLC chloride channels and transporters. Curr Opin Neurobiol 15:319–325
15. Accardi A, Miller C (2004) Secondary active transport mediated by a prokaryotic homologue of ClC Cl^- channels. Nature 427:803–807
16. Picollo A, Pusch M (2005) Chloride/proton antiporter activity of mammalian CLC proteins ClC-4 and ClC-5. Nature 436:420–423
17. Scheel O, Zdebik AA, Lourdel S, Jentsch TJ (2005) Voltage-dependent electrogenic chloride/proton exchange by endosomal CLC proteins. Nature 436:424–427
18. Graves AR, Curran PK, Smith CL, Mindell JA (2008) The Cl^-/H^+ antiporter ClC-7 is the primary chloride permeation pathway in lysosomes. Nature 453:788–792
19. Lange PF, Wartosch L, Jentsch TJ, Fuhrmann JC (2006) ClC-7 requires Ostm1 as a beta-subunit to support bone resorption and lysosomal function. Nature 440:220–223
20. Balemans W, Van Wesenbeeck L, Van Hul W (2005) A clinical and molecular overview of the human osteopetroses. Calcif Tissue Int 77:263–274
21. Helfrich MH (2003) Osteoclast diseases. Microsc Res Tech 61:514–532
22. Ogbureke KU, Zhao Q, Li YP (2005) Human osteopetroses and the osteoclast V-H^+-ATPase enzyme system. Front Biosci 10:2940–2954
23. Tolar J, Teitelbaum SL, Orchard PJ (2004) Osteopetrosis. N Engl J Med 351:2839–2849
24. Frattini A, Pangrazio A, Susani L, Sobacchi C, Mirolo M, Abinun M, Andolina M, Flanagan A, Horwitz EM, Mihci E, Notarangelo LD, Ramenghi U, Teti A, Van Hove J, Vujic D, Young T, Albertini A, Orchard PJ, Vezzoni P, Villa A (2003) Chloride channel ClCN7 mutations are responsible for severe recessive, dominant, and intermediate osteopetrosis. J Bone Miner Res 18:1740–1747
25. Alatalo SL, Ivaska KK, Waguespack SG, Econs MJ, Vaananen HK, Halleen JM (2004) Osteoclast-derived serum tartrate-resistant acid phosphatase 5b in Albers-Schonberg disease (type II autosomal dominant osteopetrosis). Clin Chem 50:883–890
26. Bollerslev J, Steiniche T, Melsen F, Mosekilde L (1989) Structural and histomorphometric studies of iliac crest trabecular and

cortical bone in autosomal dominant osteopetrosis: a study of two radiological types. Bone 10:19–24
27. Del Fattore A, Peruzzi B, Rucci N, Recchia I, Cappariello A, Longo M, Fortunati D, Ballanti P, Iacobini M, Luciani M, Devito R, Pinto R, Caniglia M, Lanino E, Messina C, Cesaro S, Letizia C, Bianchini G, Fryssira H, Grabowski P, Shaw N, Bishop N, Hughes D, Kapur RP, Datta HK, Taranta A, Fornari R, Migliaccio S, Teti A (2006) Clinical, genetic, and cellular analysis of 49 osteopetrotic patients: implications for diagnosis and treatment. J Med Genet 43:315–325
28. Karsdal MA, Martin TJ, Bollerslev J, Christiansen C, Henriksen K (2007) Are nonresorbing osteoclasts sources of bone anabolic activity? J Bone Miner Res 22:487–494
29. Karsdal MA, Henriksen K, Sorensen MG, Gram J, Schaller S, Dziegiel MH, Heegaard AM, Christophersen P, Martin TJ, Christiansen C, Bollerslev J (2005) Acidification of the osteoclastic resorption compartment provides insight into the coupling of bone formation to bone resorption. Am J Pathol 166:467–476
30. Karsdal MA, Neutzsky-Wulff AV, Dziegiel MH, Christiansen C, Henriksen K (2008) Osteoclasts secrete non-bone derived signals that induce bone formation. Biochem Biophys Res Commun 366:483–488
31. Martin TJ, Sims NA (2005) Osteoclast-derived activity in the coupling of bone formation to resorption. Trends Mol Med 11:76–81
32. Kasper D, Planells-Cases R, Fuhrmann JC, Scheel O, Zeitz O, Ruether K, Schmitt A, Poet M, Steinfeld R, Schweizer M, Kornak U, Jentsch TJ (2005) Loss of the chloride channel ClC-7 leads to lysosomal storage disease and neurodegeneration. EMBO J 24:1079–1091
33. Winding B, NicAmhlaoibh R, Misander H, Hoegh-Andersen P, Andersen TL, Holst-Hansen C, Heegaard AM, Foged NT, Brunner N, Delaisse JM (2002) Synthetic matrix metalloproteinase inhibitors inhibit growth of established breast cancer osteolytic lesions and prolong survival in mice. Clin Cancer Res 8:1932–1939
34. Ridnour LA, Windhausen AN, Isenberg JS, Yeung N, Thomas DD, Vitek MP, Roberts DD, Wink DA (2007) Nitric oxide regulates matrix metalloproteinase-9 activity by guanylyl-cyclase-dependent and -independent pathways. Proc Natl Acad Sci USA 104:16898–16903
35. Sondergaard BC, Henriksen K, Wulf H, Oestergaard S, Schurigt U, Brauer R, Danielsen I, Christiansen C, Qvist P, Karsdal MA (2006) Relative contribution of matrix metalloprotease and cysteine protease activities to cytokine-stimulated articular cartilage degradation. Osteoarthritis Cartilage 14:738–748
36. Edwards JC, Cohen C, Xu W, Schlesinger PH (2006) c-Src control of chloride channel support for osteoclast HCl transport and bone resorption. J Biol Chem 281:28011–28022
37. Sorensen MG, Henriksen K, Neutzsky-Wulff AV, Dziegiel MH, Karsdal MA (2007) Diphyllin, a novel and naturally potent V-ATPase inhibitor, abrogates acidification of the osteoclastic resorption lacunae and bone resorption. J Bone Miner Res 22:1640–1648
38. Henriksen K, Karsdal M, Delaisse JM, Engsig MT (2003) RANKL and vascular endothelial growth factor (VEGF) induce osteoclast chemotaxis through an ERK1/2-dependent mechanism. J Biol Chem 278:48745–48753
39. Karsdal MA, Hjorth P, Henriksen K, Kirkegaard T, Nielsen KL, Lou H, Delaisse JM, Foged NT (2003) Transforming growth factor-beta controls human osteoclastogenesis through the p38 MAPK and regulation of RANK expression. J Biol Chem 278:44975–44987
40. Henriksen K, Gram J, Høegh-Andersen P, Jemtland R, Ueland T, Dziegiel MH, Schaller S, Bollerslev J, Karsdal MA (2005) Osteoclasts from patients with autosomal dominant osteopetrosis type I caused by a T253I mutation in low-density lipoprotein receptor-related protein 5 are normal in vitro, but have decreased resorption capacity in vivo. Am J Pathol 167:1341–1348
41. Henriksen K, Tanko LB, Qvist P, Delmas PD, Christiansen C, Karsdal MA (2007) Assessment of osteoclast number and function: application in the development of new and improved treatment modalities for bone diseases. Osteoporos Int 18:681–685
42. Cleiren E, Benichou O, Van Hul E, Gram J, Bollerslev J, Singer FR, Beaverson K, Aledo A, Whyte MP, Yoneyama T, De Vernejoul MC, Van Hul W (2001) Albers-Schonberg disease (autosomal dominant osteopetrosis, type II) results from mutations in the ClCN7 chloride channel gene. Hum Mol Genet 10:2861–2867
43. Waguespack SG, Koller DL, White KE, Fishburn T, Carn G, Buckwalter KA, Johnson M, Kocisko M, Evans WE, Foroud T, Econs MJ (2003) Chloride channel 7 (ClCN7) gene mutations and autosomal dominant osteopetrosis, type II. J Bone Miner Res 18:1513–1518
44. Henriksen K, Gram J, Schaller S, Dahl BH, Dziegiel MH, Bollerslev J, Karsdal MA (2004) Characterization of osteoclasts from patients harboring a G215R mutation in ClC-7 causing autosomal dominant osteopetrosis type II. Am J Pathol 164:1537–1545
45. Chu K, Snyder R, Econs MJ (2006) Disease status in autosomal dominant osteopetrosis type 2 is determined by osteoclastic properties. J Bone Miner Res 21:1089–1097
46. Blair HC, Borysenko CW, Villa A, Schlesinger PH, Kalla SE, Yaroslavskiy BB, Garcia-Palacios V, Oakley JI, Orchard PJ (2004) In vitro differentiation of CD14 cells from osteopetrotic subjects: contrasting phenotypes with TCIRG1, CLCN7, and attachment defects. J Bone Miner Res 19:1329–1338
47. Letizia C, Taranta A, Migliaccio S, Caliumi C, Diacinti D, Delfini E, D'Erasmo E, Iacobini M, Roggini M, Albagha OM, Ralston SH, Teti A (2004) Type II benign osteopetrosis (Albers-Schonberg disease) caused by a novel mutation in CLCN7 presenting with unusual clinical manifestations. Calcif Tissue Int 74:42–46
48. Nielsen RH, Karsdal MA, Sorensen MG, Dziegiel MH, Henriksen K (2007) Dissolution of the inorganic phase of bone leading to release of calcium regulates osteoclast survival. Biochem Biophys Res Commun 360:834–839
49. Bollerslev J, Marks SC Jr, Pockwinse S, Kassem M, Brixen K, Steiniche T, Mosekilde L (1993) Ultrastructural investigations of bone resorptive cells in two types of autosomal dominant osteopetrosis. Bone 14:865–869
50. Blair HC, Teitelbaum SL, Tan HL, Koziol CM, Schlesinger PH (1991) Passive chloride permeability charge coupled to H^+-ATPase of avian osteoclast ruffled membrane. Am J Physiol Cell Physiol 260:C1315–C1324
51. Schaller S, Henriksen K, Sveigaard C, Heegaard AM, Helix N, Stahlhut M, Ovejero MC, Johansen JV, Solberg H, Andersen TL, Hougaard D, Berryman M, Shiodt CB, Sorensen BH, Lichtenberg J, Christophersen P, Foged NT, Delaisse JM, Engsig MT, Karsdal MA (2004) The chloride channel inhibitor n53736 prevents bone resorption in ovariectomized rats without changing bone formation. J Bone Miner Res 19:1144–1153
52. Graves AR, Curran PK, Smith CL, Mindell JA (2008) The Cl^-/H^+ antiporter ClC-7 is the primary chloride permeation pathway in lysosomes. Nature 453:788–792
53. Garnero P, Ferreras M, Karsdal MA, NicAmhlaoibh R, Risteli J, Borel O, Qvist P, Delmas PD, Foged NT, Delaisse JM (2003) The type I collagen fragments ICTP and CTX reveal distinct enzymatic pathways of bone collagen degradation. J Bone Miner Res 18:859–867

54. Kiviranta R, Morko J, Alatalo SL, NicAmhlaoibh R, Risteli J, Laitala-Leinonen T, Vuorio E (2005) Impaired bone resorption in cathepsin K-deficient mice is partially compensated for by enhanced osteoclastogenesis and increased expression of other proteases via an increased RANKL/OPG ratio. Bone 36:159–172

55. Delaisse JM, Engsig MT, Everts V, del Carmen OM, Ferreras M, Lund L, Vu TH, Werb Z, Winding B, Lochter A, Karsdal MA, Troen T, Kirkegaard T, Lenhard T, Heegaard AM, Neff L, Baron R, Foged NT (2000) Proteinases in bone resorption: obvious and less obvious roles. Clin Chim Acta 291:223–234